


# Porous Siloxane–Organic Hybrid with Ultrahigh Surface Area through Simultaneous Polymerization—Destruction of Functionalized Cubic Siloxane Cages

Watcharop Chaikittisilp,<sup>†</sup> Masaru Kubo, Takahiko Moteki, Ayae Sugawara-Narutaki, Atsushi Shimojima, and Tatsuya Okubo\*

Department of Chemical System Engineering, The University of Tokyo, 7-3-1 Hongo, Bunkyo-ku, Tokyo 113-8656, Japan

 Supporting Information

**ABSTRACT:** A novel hierarchically porous, hyper-cross-linked siloxane–organic hybrid (PSN-5) has been synthesized by Friedel–Crafts self-condensation of benzyl chloride-terminated double-four-ring cubic siloxane cages as a singular molecular precursor. Simultaneous polymerization of the organic functional groups and destruction of the siloxane cages during synthesis yielded PSN-5, which has an ultrahigh BET surface area ( $\sim 2500 \text{ m}^2 \text{ g}^{-1}$ ) and large pore volume ( $\sim 3.3 \text{ cm}^3 \text{ g}^{-1}$ ) that to our knowledge are the highest values reported for siloxane-based materials. PSN-5 also shows a high  $\text{H}_2$  uptake of 1.25 wt % at 77 K and 760 Torr.

The designed synthesis of a priori nanomaterials with tailor-made structures and properties is a scientific and technological challenge in materials science and engineering. Bottom-up assembly of well-defined molecular building blocks has settled at the center of synthetic chemistry as a strategic proposition for the construction of novel nanoporous architectures.<sup>1</sup> Ideally, such strategic building blocks should possess geometric restrictions to structure-direct the formation of objective frameworks. In addition, advantageous functionalities can be introduced into the frameworks by using building blocks bearing desired functional groups.<sup>2</sup> Because of the growing need for functional porous materials for emerging applications such as heterogeneous green catalysis, gas storage and separation, light harvesting, and drug delivery, the synthesis of highly porous inorganic–organic hybrids has advanced considerably over the past decade.<sup>2–4</sup> In particular, organically functionalized silica has been achieved mostly via postsynthetic grafting of functional silanes onto silica surfaces, direct co-condensation of molecular silanes during synthesis, and use of bridged organosilanes as precursors.

Alternatively, porous siloxane-based hybrids can be obtained from organic derivatives of double-four-ring (D4R) siloxane units through Si–O–Si, Si–C, or C–C bond formation between the units.<sup>5–8</sup> In comparison with conventional monomeric precursors, such designed D4R precursors can provide better control over the structures and properties of the resulting materials. We recently succeeded in synthesizing poly(organosiloxane) networks (PSNs) with apparent Brunauer–Emmet–Teller (BET) specific surface areas of up to  $1050 \text{ m}^2 \text{ g}^{-1}$  via coupling reactions of bromophenylethynyl-terminated D4R cages.<sup>7</sup> On the basis of pore size distributions and solid-state NMR analyses, the local

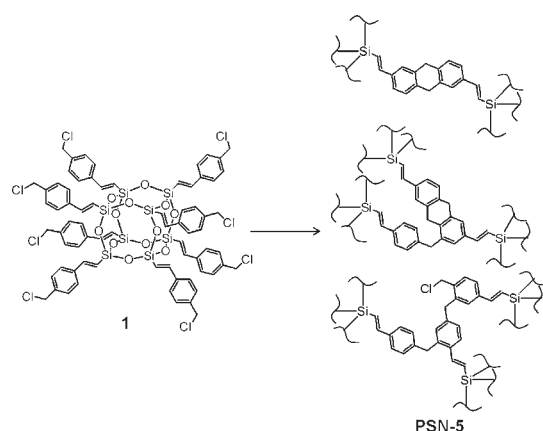
networks of the resulting hybrids (PSN-1–4) were formed in an orderly fashion from the retained D4R cages.<sup>7</sup> More importantly, one hybrid in this PSN series, PSN-4, exhibited a certain degree of crystallinity and appears to be one of the first polymer networks possessing some crystallinity even though it was produced by an irreversible reaction.<sup>7b</sup> In contrast to conventional methods, in this case organic moieties were used to assemble the networks.<sup>2,7,8</sup> However, their BET surface areas did not exceed the highest value reported for a siloxane-based hybrid (i.e.,  $1880 \text{ m}^2 \text{ g}^{-1}$  for a phenylene-bridged polysilsesquioxane aerogel<sup>9</sup>).

PSN materials with higher surface areas can be more useful because they should have more accessible organic functional groups. Inspired by the recent development of microporous hyper-cross-linked polymers,<sup>10</sup> we surmised that such higher surface area, porous siloxane–organic hybrid materials could be achieved by increasing the degree of cross-linking of the organic moieties. Indeed, previous reports on microporous hyper-cross-linked organic polymers and PSNs have suggested that the higher level of cross-linking and hence higher network rigidity can lead to higher surface areas for the resulting materials.<sup>7a,10b,10c</sup> We describe herein a simple approach for producing highly porous siloxane-based inorganic–organic hybrids by Friedel–Crafts self-condensation of benzyl chloride-terminated D4R siloxane **1** as a singular molecular precursor. A similar reaction has recently been used to prepare porous cross-linked organic polymers.<sup>10b,d</sup> By using the D4R-based precursor, we achieved an extremely high surface area that is attributable to (i) a highly connectable or hyperbranched feature of the D4R cages that should intensify the hyper-cross-linking of the network and (ii) substantial cleavage of the D4R cages to form less-dense siloxane units during the reaction, possibly as a result of cage distortion in the hyper-cross-linked networks.

As shown in Scheme 1, the hybrid PSN-5 was synthesized by Friedel–Crafts alkylation of **1** in the presence of Lewis acid catalysts. The network of hyper-cross-linked polymers was typically formed in a random fashion.<sup>10</sup> Some possible fragments of the resulting PSN-5 are shown as examples in Scheme 1. Briefly, precursor **1** was first synthesized by cross-metathesis and purified by gel permeation chromatography (for details, see the Supporting Information).<sup>7,11</sup> Friedel–Crafts alkylation was carried out at 85 °C in 1,2-dichloroethane for 25 h in the presence of  $\text{FeCl}_3$  (PSN-Sa) or  $\text{AlCl}_3$  (PSN-Sb) as the catalyst. The resulting

Received: May 20, 2011

Published: August 05, 2011

**Scheme 1. Synthesis of PSN-5 by Friedel–Crafts Self-Condensation of 1<sup>a</sup>**


<sup>a</sup> Only some of the possible fragments of PSN-5 are shown as examples.

PSN-5 was then recovered by filtration, successively washed with several solvents, and dried under vacuum.

PSN-5a was prepared using FeCl<sub>3</sub>, which is the most frequently used Lewis acid catalyst for preparing microporous hyper-cross-linked polymers.<sup>10,12</sup> Energy-dispersive X-ray fluorescence (XRF) spectroscopy revealed that the FeCl<sub>3</sub>-catalyzed Friedel–Crafts alkylation did not go to completion under the investigated conditions. The Cl/Si molar ratio of PSN-5a was ~0.5, which is equivalent to 50% conversion. The Fe/Si molar ratio was less than 0.0005, indicating that most of the iron catalyst was removed during the workup procedure. To increase the conversion, the amount of catalyst was doubled; however, the conversion was essentially unchanged under otherwise identical conditions. Therefore, we used another common Lewis catalyst, AlCl<sub>3</sub>. PSN-5b was synthesized under the same conditions as for PSN-5a except for the catalyst used. Neither chlorine end groups nor residual aluminum catalyst was observable by XRF analysis, suggesting that in the case of PSN-5b, the reaction was nearly complete. In addition, the difference in the conversion of PSN-5 samples was confirmed by FT-IR spectroscopy. The IR wagging vibration band of the chloromethyl group (–CH<sub>2</sub>Cl)<sup>12</sup> at 1265 cm<sup>–1</sup> was observed for the PSN-5a sample but not noticeable for the PSN-5b material (Figure S1 in the Supporting Information).

The progress of the reaction was also confirmed by solid-state <sup>1</sup>H–<sup>13</sup>C cross-polarization/magic-angle-spinning (CP/MAS) NMR spectroscopy. As shown in Figure 1a, the signals arising from C<sub>AR</sub>–C, C<sub>AR</sub>–H, CH<sub>2</sub>Cl, and CH<sub>2</sub> were observed at ca. 139, 127, 43, and 38 ppm, respectively. The increased peak ratio of substituted and nonsubstituted aromatic carbons (C<sub>AR</sub>–C/C<sub>AR</sub>–H) as well as the presence of CH<sub>2</sub> carbons confirmed the formation of C–C bonds. In addition, the signals arising from two ethylene carbons would appear at ca. 149 and 118 ppm as the shoulders of the aromatic signals, although they were unclear because of the broadness of the spectra (see Figure S2 for peak fittings). Solid-state <sup>29</sup>Si MAS NMR spectra (Figure 1b) revealed local structural information concerning the siloxane networks. Unlike the PSN hybrids reported previously,<sup>7</sup> the spectra unexpectedly revealed signals at ca. –69 and –79 ppm, which were assigned to T<sup>2</sup> and T<sup>3</sup> units, respectively [T<sup>n</sup> = CSi(OSi)<sub>n–1</sub>(OH)<sub>3–n</sub>], with a relatively low T<sup>3</sup>/(T<sup>2</sup> + T<sup>3</sup>) ratio of 0.34, indicating that during the synthesis, destruction of the D4R units

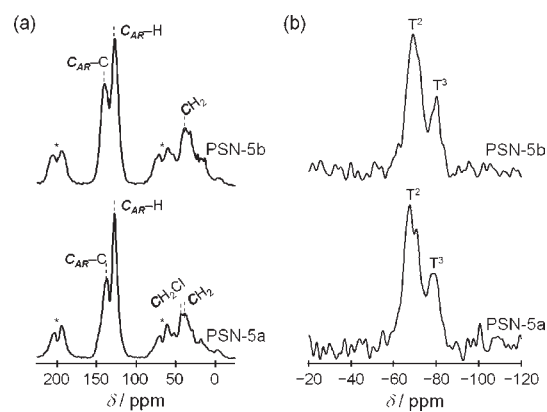


**Figure 1.** Solid-state (a) <sup>1</sup>H–<sup>13</sup>C CP/MAS and (b) <sup>29</sup>Si MAS NMR spectra of PSN-5 hybrids obtained from Friedel–Crafts alkylation catalyzed by FeCl<sub>3</sub> (PSN-5a; bottom) and AlCl<sub>3</sub> (PSN-5b; top). Asterisks denote spinning sidebands.

occurred simultaneously with the polymerization of the organic functional groups. This was probably due to the structural distortion of polymerized 1 and the acids used in and released from the reaction. Previously, such a structural distortion of D4R cages was suggested to occur to reduce the structural constraints or stresses of the resulting networks when the D4R cages were connected together by rigid linking units.<sup>7a</sup> It is also noteworthy that molecular D4R cages were retained when they were functionalized without cross-linking by means of AlCl<sub>3</sub>-catalyzed Friedel–Crafts reactions, although the functionalization was carried out under much milder conditions.<sup>13</sup> We have considered that the siloxane units can connect together more effectively because of this unexpected destruction of 1, subsequently resulting in more highly cross-linked materials with higher surface areas. In addition, the presence of silanol groups (T<sup>2</sup> silicons) can be useful for further postsynthetic modifications (e.g., by silylation).

The thermal stability of the resulting networks was examined by thermogravimetric analysis (TGA) and differential thermal analysis. The PSN-5b hybrid was stable up to ca. 400 °C, which was ca. 20 degrees higher than PSN-5a (Figure S3). Small-angle powder X-ray diffraction (PXRD) patterns of both PSN-5 hybrids (Figure S4) exhibited a broad XRD peak centered at a 2θ value of ca. 2°, probably reflecting the presence of mesopores and/or aggregated small nanoparticles. The obtained hybrids had irregular shapes with sizes of 3–10 μm and rough surfaces, as observed by field-emission scanning electron microscopy (FE-SEM; Figure S5). As shown in Figure 2, translucent high-resolution transmission electron microscopy (HRTEM) images indicate the porous characteristics of the PSN-5 samples. The presence of micropores is evident.

The existence of micro- and mesopores in the PSN-5 hybrids was directly corroborated by N<sub>2</sub> physisorption measurements. Figure 3a shows the N<sub>2</sub> adsorption–desorption isotherms of the resulting hybrids. The samples showed sharp uptake at low relative pressures and gradually increasing uptake at higher relative pressures with small hysteresis, indicating that the PSN-5 hybrids contained both micro- and mesopores. The BET method was applied to determine the surface areas of the PSN-5 hybrids. Because the materials contained micropores, the pressure range selected for calculation of the surface area had to have values of  $v(P_0 - P)$  (where  $v$  is the adsorbed volume of N<sub>2</sub>) that increased continuously with  $P/P_0$  in addition to a linear BET plot and a

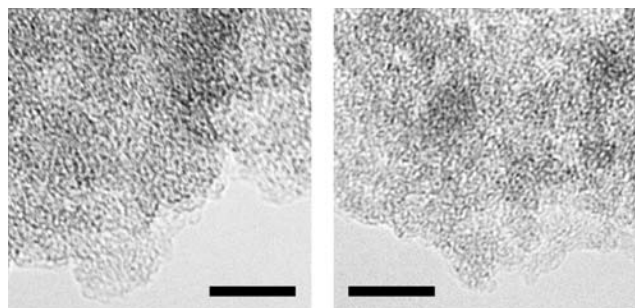


**Figure 2.** HRTEM images of (left) PSN-5a and (right) PSN-5b (scale bars: 10 nm). Notably, the samples were very stable under the electron beam.

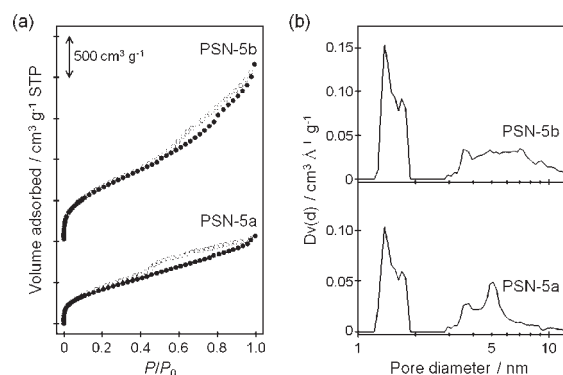


**Figure 3.** (a)  $N_2$  adsorption–desorption isotherms (solid and open symbols represent adsorption and desorption branches, respectively). The isotherm of PSN-5b has been shifted vertically by  $1000 \text{ cm}^3 \text{ g}^{-1}$  STP. (b) NLDFT pore size distributions of PSN-5a (bottom) and PSN-5b (top).

positive value of the  $c$  parameter.<sup>14</sup> As shown in Figure S6, the PSN-5 hybrids exhibited continuous increases in  $v(P_0 - P)$  up to  $P/P_0 = 0.23$ – $0.30$  depending on the sample, suggesting that to satisfy the criterion, only a range of relative pressures less than these  $P/P_0$  values could be considered in the BET analysis. In particular, the BET surface areas of the PSN-5 hybrids were calculated using the range  $P/P_0 = 0.05$ – $0.15$ , in which the BET plots satisfied all the major criteria, namely, BET plot linearity, positive  $c$  value, and increasing  $v(P_0 - P)$ . To confirm the reproducibility of the materials synthesis, PSN-5 hybrids were synthesized under the exactly same conditions at least twice, and  $N_2$  physisorption of each sample was measured twice (see the BET plots in Figure S6). PSN-5a synthesized with the  $\text{FeCl}_3$  catalyst, which showed lower activity under the investigated conditions, exhibited an apparent BET specific surface area of  $1576 \pm 34 \text{ m}^2 \text{ g}^{-1}$  and a total pore volume (at  $P/P_0 = 0.99$ ) of  $1.68 \pm 0.05 \text{ cm}^3 \text{ g}^{-1}$ . Unprecedentedly, PSN-5b obtained using the  $\text{AlCl}_3$  catalyst exhibited the incredibly high apparent BET specific surface area of  $2509 \pm 59 \text{ m}^2 \text{ g}^{-1}$  and the large total pore volume (at  $P/P_0 = 0.99$ ) of  $3.28 \pm 0.10 \text{ cm}^3 \text{ g}^{-1}$ , which are among the highest values reported to date for siloxane-based porous solids.<sup>2–9</sup> In comparison with styrenic hyper-cross-linked polymers having cross-linking groups similar to those of the PSN-5 hybrids, the surface area of PSN-5b also exceeded the highest BET surface area reported to date for such materials ( $2090 \text{ m}^2 \text{ g}^{-1}$ ).<sup>12a</sup> The lower surface area of PSN-5a relative to PSN-5b can be ascribed to the lower degree of organic polymerization,

as the two materials showed similar levels of the D4R cage destruction. This is consistent with previous reports showing that the degree of cross-linking (that is, the efficiency in condensation reactions) strongly affects the surface area of the resulting network.<sup>7a,10b,10c</sup>

In the porous siloxane-based hybrids obtained by conventional sol–gel chemistry, including bridged polysilsesquioxane gels and periodic mesoporous organosilicas, polycondensation of silsesquioxane moieties in monomeric and oligomeric precursors tends to form dense silica matrixes, as such densification is responsible for stabilizing the porous frameworks.<sup>2,3,5</sup> As a result, the surface areas of such hybrids are limited to a certain value. In the case of PSN-5, on the contrary, the porous networks are constructed by the condensation of the organic groups and simultaneous destruction of the siloxane parts, and therefore, the formation of dense silica and organic matrixes is prevented. The hyperbranched characteristic of the cleaved D4R cages together with the hyper-cross-linked feature of the organic groups yield the ultrahigh surface area of the PSN-5 networks.

Pore size distributions of the hybrids were calculated using nonlocal density functional theory (NLDFT). As shown in Figure 3b, the PSN-5 materials possess fairly uniform micropores with a diameter of 1.4 nm and a shoulder at 1.7 nm. PSN-5b shows a relatively broad distribution of mesopores, while PSN-5a has more uniform mesopores with predominant diameters at 3.7 and 5.0 nm. In the case of PSN-5a, the mesopore size distribution was also determined from the desorption branch of the isotherm using the Barrett–Joyner–Halenda (BJH) method, which revealed a narrow distribution at 3.7 nm. These mesopores can allow several molecules to diffuse into and further react with silanol groups during postmodification. It is noteworthy that the pore size distribution of polymer-type porous networks, including the PSN-5 hybrids, should be carefully determined because of the disordered nature of the materials and the pressure-dependent structural changes of some porous polymers.<sup>15</sup>

$H_2$  adsorption capacities of the PSN-5 hybrids were evaluated at 77 and 87 K by a volumetric method. The  $H_2$  uptakes for PSN-5a and PSN-5b at 77 K and 760 Torr were 1.19 and 1.25 wt %, respectively (Figure S7). The isosteric heats of adsorption at low  $H_2$  coverage were calculated to be 8.3 and 8.1  $\text{kJ mol}^{-1}$  for PSN-5a and PSN-5b, respectively. Their  $H_2$  uptakes and heats of adsorption are similar to those of promising candidates for  $H_2$  storage applications, such as metal–organic frameworks and porous organic frameworks.<sup>7,10,16</sup>

In summary, a hierarchically micro- and mesoporous hyper-cross-linked siloxane–organic hybrid material has been synthesized by self-condensation of benzyl chloride-terminated cubic siloxane cages via Friedel–Crafts alkylation. The obtained PSN-5 hybrids exhibit ultrahigh surface areas and large pore volumes. To our knowledge, in comparison with other siloxane-based porous solids and styrenic hyper-cross-linked polymers reported previously, PSN-5 shows the highest BET surface area, ca.  $2500 \text{ m}^2 \text{ g}^{-1}$ . Although the siloxane cages collapse during synthesis, this benzyl chloride-terminated unit can serve as a good and singular precursor for the construction of hyper-cross-linked porous networks with extremely high surface areas and large pore volumes. This finding suggests that *simultaneous* polymerization of organic functional groups and destruction of the siloxane cages would be a strategic concept in the construction of highly porous siloxane–organic hybrids. However, the destruction mechanism is still unclear, and a more complete understanding is necessary to gain better control over the synthesis and

subsequent properties of the resulting hybrids. Future studies such as investigations of the local siloxane structures of the intermediate products using quantitative solid-state NMR and advanced synchrotron X-ray analyses are anticipated.

## ■ ASSOCIATED CONTENT

**S Supporting Information.** Experimental details, FT-IR spectra, fits of  $^1\text{H}$ – $^{13}\text{C}$  CP/MAS NMR spectra, TGA results, PXRD patterns, FE-SEM images,  $\nu(P_0 - P)$  and BET plots, and  $\text{H}_2$  adsorption results. This material is available free of charge via the Internet at <http://pubs.acs.org>.

## ■ AUTHOR INFORMATION

### Corresponding Author

okubo@chemsys.t.u-tokyo.ac.jp

### Present Addresses

<sup>†</sup>School of Chemical & Biomolecular Engineering, Georgia Institute of Technology, 311 Ferst Drive, Atlanta, GA 30332, USA. E-mail: [watcharop@chbe.gatech.edu](mailto:watcharop@chbe.gatech.edu).

## ■ ACKNOWLEDGMENT

We are grateful to Prof. S. Maruyama for access to the FE-SEM instrument. This study was supported in part by a Grant-in-Aid for Scientific Research (B) from the Japan Society for the Promotion of Science (JSPS) and by a Global COE Program (Mechanical Systems Innovation) from the Ministry of Education, Culture, Sports, Science and Technology (MEXT), Japan. W.C. thanks MEXT for a Monbukagakusho Scholarship. M.K. and T.M. are JSPS Fellows (DC1). A part of this work was conducted at the Center for Nano Lithography & Analysis at The University of Tokyo, which is supported by MEXT.

## ■ REFERENCES

- (1) (a) Davis, M. E. *Nature* **2002**, *417*, 813. (b) Shimojima, A.; Kuroda, K. *Chem. Rec.* **2006**, *6*, 53. (c) Burton, A. W. *J. Am. Chem. Soc.* **2007**, *129*, 7627. (d) Alkordi, M. H.; Brant, J. A.; Wojtas, L.; Kravtsov, V. Ch.; Cairns, A. J.; Eddaoudi, M. *J. Am. Chem. Soc.* **2009**, *131*, 17753.
- (2) Thomas, A. *Angew. Chem., Int. Ed.* **2010**, *49*, 8328.
- (3) (a) Hoffmann, F.; Cornelius, M.; Morell, J.; Fröba, M. *Angew. Chem., Int. Ed.* **2006**, *45*, 3216. (b) Fujita, S.; Inagaki, S. *Chem. Mater.* **2008**, *20*, 891. (c) Shea, K. J.; Loy, D. A. *Chem. Mater.* **2001**, *13*, 3306. (d) Nakanishi, K.; Tanaka, N. *Acc. Chem. Res.* **2007**, *40*, 863.
- (4) (a) McKittrick, M. W.; Jones, C. W. *Chem. Mater.* **2003**, *15*, 1132. (b) Zhang, Q.; Ariga, K.; Okabe, A.; Aida, T. *J. Am. Chem. Soc.* **2004**, *126*, 988. (c) Yokoi, T.; Yoshitake, H.; Yamada, T.; Kubota, Y.; Tatsumi, T. *J. Mater. Chem.* **2006**, *16*, 1125. (d) MacQuarrie, S.; Thompson, M. P.; Blanc, A.; Mosey, N. J.; Lemieux, R. P.; Crudden, C. M. *J. Am. Chem. Soc.* **2008**, *130*, 14099. (e) Kanezashi, M.; Yada, K.; Yoshioka, T.; Tsuru, T. *J. Am. Chem. Soc.* **2009**, *131*, 414. (f) Mizoshita, N.; Ikai, M.; Tani, T.; Inagaki, S. *J. Am. Chem. Soc.* **2009**, *131*, 14225. (g) Gu, J.; Fan, W.; Shimojima, A.; Okubo, T. *Small* **2007**, *3*, 1740. (h) Fertier, L.; Théron, C.; Carcel, C.; Trens, P.; Wong Chi Man, M. *Chem. Mater.* **2011**, *23*, 2100.
- (5) (a) Hagiwara, Y.; Shimojima, A.; Kuroda, K. *Chem. Mater.* **2008**, *20*, 1147. (b) Goto, R.; Shimojima, A.; Kuge, H.; Kuroda, K. *Chem. Commun.* **2008**, 6152. (c) Zhang, L.; Abbenhuis, H. C. L.; Yang, Q.; Wang, Y.-M.; Magusin, P. C. M. M.; Mezari, B.; van Santen, R. A.; Li, C. *Angew. Chem., Int. Ed.* **2007**, *46*, 5003.
- (6) (a) Hoebbel, D.; Endres, K.; Reinert, T.; Pitsch, I. *J. Non-Cryst. Solids* **1994**, *176*, 179. (b) Zhang, C.; Babonneau, F.; Bonhomme, C.

Laine, R. M.; Soles, C. L.; Hristov, H. A.; Yee, A. F. *J. Am. Chem. Soc.* **1998**, *120*, 8380.

(7) (a) Chaikittisilp, W.; Sugawara, A.; Shimojima, A.; Okubo, T. *Chem.—Eur. J.* **2010**, *16*, 6006. (b) Chaikittisilp, W.; Sugawara, A.; Shimojima, A.; Okubo, T. *Chem. Mater.* **2010**, *22*, 4841.

(8) (a) Roll, M. F.; Kampf, J. W.; Kim, Y.; Yi, E.; Laine, R. M. *J. Am. Chem. Soc.* **2010**, *132*, 10171. (b) Kim, Y.; Koh, K.; Roll, M. F.; Laine, R. M.; Matzger, A. J. *Macromolecules* **2010**, *43*, 6995.

(9) Schaefer, D. W.; Beaucage, G.; Loy, D. A.; Shea, K. J.; Lin, J. S. *Chem. Mater.* **2004**, *16*, 1402.

(10) (a) Germain, J.; Hradil, J.; Fréchet, J. M. J.; Svec, F. *Chem. Mater.* **2006**, *18*, 4430. (b) Wood, C. D.; Tan, B.; Trewin, A.; Niu, H.; Bradshaw, D.; Rosseinsky, M. J.; Khimyak, Y. Z.; Campbell, N. L.; Kirk, R.; Stöckel, E.; Cooper, A. I. *Chem. Mater.* **2007**, *19*, 2034. (c) Tsyurupa, M. P.; Davankov, V. A. *React. Funct. Polym.* **2006**, *66*, 768. (d) Li, B.; Gong, R.; Wang, W.; Huang, X.; Zhang, W.; Li, H.; Hu, C.; Tan, B. *Macromolecules* **2011**, *44*, 2410.

(11) (a) Itami, Y.; Marciniak, B.; Kubicki, M. *Chem.—Eur. J.* **2004**, *10*, 1239. (b) Cheng, G.; Vautravers, N. R.; Morris, R. E.; Cole-Hamilton, D. J. *Org. Biomol. Chem.* **2008**, *6*, 4662.

(12) (a) Ahn, J.-H.; Jang, J.-E.; Oh, C.-G.; Ihm, S.-K.; Cortez, J.; Sherrington, D. C. *Macromolecules* **2006**, *39*, 627. (b) Schwab, M. G.; Senkova, I.; Rose, M.; Klein, N.; Koch, M.; Pahnke, J.; Jonschker, G.; Schmitz, B.; Hirscher, M.; Kaskel, S. *Soft Matter* **2009**, *5*, 1055.

(13) Kawakami, Y.; Kabe, Y. *Chem. Lett.* **2010**, *39*, 1082.

(14) (a) Rouquerol, J.; Llewellyn, P.; Rouquerol, F. *Stud. Surf. Sci. Catal.* **2007**, *160*, 49. (b) Walton, K. S.; Snurr, R. Q. *J. Am. Chem. Soc.* **2007**, *129*, 8552.

(15) Weber, J.; Antonietti, M.; Thomas, A. *Macromolecules* **2008**, *41*, 2880.

(16) (a) Rowsell, J. L. C.; Yaghi, O. M. *Angew. Chem., Int. Ed.* **2005**, *44*, 4670. (b) Murray, L. J.; Dincă, M.; Long, J. R. *Chem. Soc. Rev.* **2009**, *38*, 1294.